THE JOURNAL OF BIOLOGICAL CHEMISTRY
Vol. 276, No. 39, Issue of September 28, pp. 36543–36549, 2001

Printed in U.S.A.

Analysis of the Pore of the Unusual Major Intrinsic Protein Channel, Yeast Fps1p*

Received for publication, June 1, 2001, and in revised form, July 6, 2001
Published, JBC Papers in Press, July 9, 2001, DOI 10.1074/jbc.M105045200

Roslyn M. Bill‡§, Kristina Hedfalk¶, Sara Karlgren‡, Jonathan G. L. Mullins‖, Jan Rydström, and Stefan Hohmann‡ ‡‡**

*From the Department of ‡Cell and Molecular Biology/Microbiology, Göteborg University, S-40530 Göteborg, Sweden, the Department of ¶Molecular Biotechnology, Chalmers University of Technology, S-40530 Göteborg, Sweden, the ‖Department of Biology and Health Science, University of Luton, Park Square, Luton, Bedfordshire, LU1 3JU, United Kingdom, and the **Department of Biochemistry and Biophysics, Göteborg University, S-40530 Göteborg, Sweden*

Fps1p is a glycerol efflux channel from *Saccharomyces cerevisiae*. In this atypical major intrinsic protein neither of the signature NPA motifs of the family, which are part of the pore, is preserved. To understand the functional consequences of this feature, we analyzed the pseudo-NPA motifs of Fps1p by site-directed mutagenesis and assayed the resultant mutant proteins *in vivo*. In addition, we took advantage of the fact that the closest bacterial homolog of Fps1p, *Escherichia coli* GlpF, can be functionally expressed in yeast, thus enabling the analysis in yeast cells of mutations that make this typical major intrinsic protein more similar to Fps1p. We observed that mutations made in Fps1p to "restore" the signature NPA motifs did not substantially affect channel function. In contrast, when GlpF was mutated to resemble Fps1p, all mutants had reduced activity compared with wild type. We rationalized these data by constructing models of one GlpF mutant and of the transmembrane core of Fps1p. Our model predicts that the pore of Fps1p is more flexible than that of GlpF. We discuss the fact that this may accommodate the divergent NPA motifs of Fps1p and that the different pore structures of Fps1p and GlpF may reflect the physiological roles of the two glycerol facilitators.

Major intrinsic protein (MIP)[1] channels, aquaporins and glycerol facilitators, occur in all types of organisms ranging from bacteria to humans. MIP channels mediate the gradient-driven diffusion of water, glycerol, and other uncharged compounds and certain ions across biological membranes. To date, more than 200 MIPs have been identified comprising an amazing number of isoforms expressed in different subcellular compartments and tissues, under different environmental conditions or during different developmental stages. For example, 10 genes encoding MIP channels are currently known in humans (1), 35 have been described in the plant *Arabidopsis thaliana* (2) and the nematode *Caenorhabditis elegans* has nine (3). These channel proteins are involved in biological processes as diverse as urine concentration in the mammalian kidney, (4) root development in *A. thaliana* (5, 6), and osmoregulation in *Saccharomyces cerevisiae* (7, 8).

Fps1p is a glycerol facilitator of the yeast *S. cerevisiae* (7, 8). The central importance of Fps1p in yeast osmoregulation is illustrated by the sensitivity to a hypo-osmotic shock of yeast cells in which *FPS1* has been deleted. Fps1p has also been shown to affect signal transduction in yeast osmoregulation in a fashion consistent with its role in controlling the intracellular glycerol content (9, 10). In addition, *fps1*Δ mutants both grow poorly and hyperaccumulate glycerol under anaerobic conditions when glycerol is produced for redox balancing (8). These observations establish that Fps1p primarily mediates glycerol diffusion out of the cell (11) with an energy-independent mechanism (8). Despite the fact that Fps1p can also mediate measurable glycerol influx into yeast cells, (7, 8, 12), this is probably not its physiological role because no growth defects have been found in *fps1*Δ mutants cultivated with glycerol as the sole carbon source (8). Furthermore *GUP1* and *GUP2* have recently been proposed to be involved in active transport of glycerol in yeasts (13). In contrast, the physiologically relevant role of GlpF from *Escherichia coli*, the closest bacterial homolog of Fps1p with 30.5% identity, is likely to be import of glycerol for catabolism (14, 15).

Although Fps1p (see Fig. 1) is closely related to bacterial glycerol channels such as GlpF from *E. coli*, it is so far unique in the MIP family for a number of reasons (11). For example, it has long amino- and carboxyl-terminal hydrophilic extensions, resulting in a protein of 669 amino acids, compared with 281 amino acids for GlpF. Only very few fungal MIPs, as well as *Drosophila* BIB, have such long extensions. The amino-terminal extension of Fps1p is important for the regulation of glycerol efflux by external osmolarity in yeast. Deletion of this domain renders the channel unregulated. Unregulatable, constitutively open Fps1p causes loss of glycerol from the cell and hence poor growth in high osmolarity medium (8). As an additional unique feature, neither of the signature Asn-Pro-Ala (NPA) motifs of the family in channel-forming loops B and E is fully preserved; instead they are Asn-Pro-Ser (NPS) and Asn-Leu-Ala (NLA), respectively (see Fig. 1). In fact, the sequences of only five other microbial MIPs contain motifs other than NPA. In four of these cases NPA is preserved in loop B: the presumed glycerol channel from *Enterococcus faecalis* (gef 6176) contains an NQA motif in loop E, the putative aquaporin from *Chloribium tepidum* (gct 5) has NPV, the *Botrytis cinerea* putative glycerol channel contains NPS, and the *Saccharomyces kluyveri* homolog of Fps1p has NMA (11, natchaug.labri.u-bordeaux.fr/Genolevures/Genolevures.php3). The only deviation from NPA in loop B of a microbial MIP occurs in the

* This work was supported by European Commission Contracts BIO4-CT98-0024 (to S. H. and J. R.) and FMRX-CT96-0128 (to S. H.) and by a grant from the Carl Trygger Foundation (to J. R.). The costs of publication of this article were defrayed in part by the payment of page charges. This article must therefore be hereby marked "*advertisement*" in accordance with 18 U.S.C. Section 1734 solely to indicate this fact.

§ To whom correspondence should be addressed. Tel: 46-31-773-3923; Fax: 46-31-773-2599; E-mail: roslyn.bill@gmm.gu.se.

‡‡ Special researcher supported by the Swedish Research Council.

[1] The abbreviations used are: MIP, major intrinsic protein; contig, group of overlapping clones; PCR, polymerase chain reaction; MES, 4-morpholineethanesulfonic acid.

TABLE I
Oligonucleotides used for site-directed mutagenesis of FPS1 *and* glpF

The bases underlined indicate either the result of the mutation being introduced or extensions used in gap repair to construct the loop swap mutants. The latter were designed by predicting the location of the transmembrane domains using the internet resources Prosis, TopPred2, TMPred, PhD, and DAS to produce a model of the transmembrane domain boundaries of Fpslp and GlpF, deleting the required loop sequence in glpF and replacing it with the corresponding one in *FPS1*. The bases in italics indicate restriction sites used for subcloning. The designators .f and .r indicate sense and antisense sequences, respectively.

Primer name	Primer sequence
S354A.f	TTGAATCCGGCTATTACATTAGCC
L481P.f	ACAGCAATGAATCCGGCTCGTGAT
M1.f	CACTCAGGTCCGATGTTCTTCTTGC
M2.r	TGTCAGGTCAATGTTGCTGGG
M3.r	GCGGGAATGTTTTGCGTT
M1uI.f	AACAAAACGCGTCGCTGT
RsrII.f	CCAGCGCGTGACTT*CGGTCCG*AAAGTCTTT
SexAI.r	TTCTACCCA*ACCTGGT*TTTGGGTAGATTTG
myc.f	CGCGTCGCTGGAACAAAAACTTATTTCTGAAGAAGATCTGAATTAATAAA
myc.r	CCTGGTTTATTAATTCAGATCTTCTTCAGAAATAAGTTTTTGTTCCAGCGA
A70S.f	AGGGGTTTCCG*GCGCGC*ATCTTAATCCCTCTGTTACCAT
NgoMI.r	GCACAGAAAGC*GCCGGC*AACTTGTGAA
P204L.r	AAAGACTTT*CGGACCG*AAGTCACGCGCTAGGTTCATGGCA
NgoMI.f	TCACAAGTT*GCCGGCG*CTTTCTGT
B1.r	GGAAACCCCTGCGGTCAG
B2.f	GTTATTCCTTTTATCGTT
B3.f	GCAATGGCCATCTACCTGACCGCAGGGGTTGCCATCTCAGGTGCTCAT
B4.r	GGCAACTTGTGAAACGATAAAAGGAATAACTTTCTTCAGGGGAAAACC
E1.r	TGTCAATGGGCCCATAGA
E2.f	CTGGTGCCGCTTTTCGGC
E3.f	CTGATTGCGGTCATTGGCGCATCTATGGGCTATCAGACAGGTACAGCA
E4.r	GATAGGGCCGAAAAGCGGCACCAGGAAGTAATGATGATGATGCACCCA

Salmonella typhimurium protein (contig 1308), which has an NLA motif. Unfortunately, these MIPs are incompletely characterized, and thus their transport characteristics cannot be used to aid our understanding of the structural and/or functional role(s) of these features. In this study we have therefore chosen to examine the consequences of the NPS and NLA sequences of Fps1p on channel function. This is of particular relevance to a general understanding of MIP channels because their generic NPA motifs have been shown to be integral to the formation of a continuous solute pore, the so-called "hourglass" (17), a prediction confirmed in the recently published structures of GlpF (18) and AQP1 (19).

To understand the functional consequences of their atypical sequence composition, we have probed loops B and E of Fps1p by site-directed mutagenesis and *in vivo* assay. Specifically, we have studied the consequences of "restoring" NPA motifs in Fps1p. In addition, we have taken advantage of the fact that the closest bacterial homolog of Fps1p, *E. coli* GlpF, which contains two NPA motifs, and for which a crystal structure has been published (18), can be functionally expressed in yeast (7). Hence, we have generated mutations that make this typical MIP resemble Fps1p and tested the function of these mutant proteins in the same yeast test system. We find that although Fps1p tolerates NPA in both loops B and E instead of its unusual pseudo-NPA motifs, GlpF only tolerates NPS in loop B. Changes in loop E of GlpF abolish protein function as determined in our yeast test system. We have rationalized these data by generating models of GlpF containing NPS in loop B and of the transmembrane regions of Fps1p, using the published structure of GlpF as a starting point (18). We discuss our results in the context of the pore of Fps1p having a different structure from that of GlpF. This may accommodate the divergent NPA motifs Fps1p, and moreover, the different pore structures of Fps1p and GlpF may reflect the different physiological roles of the two glycerol facilitators.

EXPERIMENTAL PROCEDURES

Yeast Strains and Growth Conditions—The *S. cerevisiae* strains used in this study were isogenic to W303-1A (20). The deletion mutant *fps1*Δ::*TRP1* was made by replacing a *Bgl*II fragment containing the *FPS1* open reading frame with a *Bam*HI fragment containing the *TRP1* gene from YDpW (21). Yeast cells were routinely grown in medium containing 2% peptone and 1% yeast extract supplemented with 2% glucose as carbon source. Selection and growth of transformants carrying a replicating plasmid was performed in yeast nitrogen base medium (YNB) (22). Plate growth assays were performed by pregrowing the cells to midlog phase in medium supplemented with 1 M sorbitol. A 10-fold serial dilution of this culture was made, and 10 μl of each dilution were spotted onto agar plates supplemented without osmoticum (hypo-osmotic shock). Growth was monitored after 2–3 days at 30 °C.

Plasmid Construction—YEp*myc-FPS1* is a 2μ *LEU2* plasmid expressing a fusion protein in which the c-*myc* epitope is attached to the carboxyl terminus of Fps1p (8). Plasmids containing point mutations in the *FPS1* gene were constructed using the megaprimer PCR (23) with YEp*myc-FPS1* as template and primers as listed in Table I. Single mutations were introduced using primers S354A.f or L481P.f. The flanking primers in each case were M1 and M2. The resultant PCR products were cleaved with *Kpn*I and *Apa*I and subcloned into YEp*myc-FPS1* that had been cleaved with the same enzymes. All constructs were fully sequenced using the BigDye Terminator Cycle Sequencing kit (Applied Biosystems). For the double mutant, two fragments were created; primers M1 and M3 were used to generate a PCR product using YEp*myc-FPS1*L481P as the template, and YEp*myc-FPS1*S354A was digested with *Nco*I. These fragments were used to transform *S. cerevisiae* using the lithium acetate method (24), and the resulting gap-repaired plasmids (25) were propagated in *E. coli* DH5α. This construct was fully sequenced using the BigDye Terminator Cycle Sequencing kit (Applied Biosystems). YEp*glpF* contains the gene encoding *E. coli* GlpF under the control of the yeast *PGK1* promoter (7). The gene was tagged at its 3′ end by using megaprimer PCR with primers MluI.f, RsrII.f, and SexAI.r (Table I) to create an *Mlu*I site at positions 833–838, yielding YEp*glpF-Mlu*I. A synthetic fragment was created by annealing the oligonucleotides myc.f and myc.r (Table I), which contain the c-*myc* sequence with appropriate 5′ overhangs, and this was subcloned into YEp*glpF-Mlu*I which had been cleaved with *Mlu*I and *Sex*AI. This procedure yielded YEp*glpFmyc*. Plasmids containing point mutations in the *glpF* gene were constructed using PCR with YEp*glpFmyc* as template and the primer pair A70S.f and NgoMI.r or P204L.r and NgoMI.f (Table I). Loop swaps were created using PCR by completely amplifying YEp*glpFmyc* except for the loop to be replaced by the corresponding sequence in *FPS1*. This corresponding *FPS1* sequence was then amplified using YEp*myc-FPS1* as template with primers containing 5′ 30-base extensions with 100% identity to the required *glpF* flanking sequence (Table I). These fragments were then used to transform *S. cerevisiae* using the lithium acetate method (24), and the re-

sulting gap-repaired plasmids (25) were propagated in *E. coli* DH5α. All constructs were fully sequenced using the BigDye Terminator Cycle Sequencing kit (Applied Biosystems). All other molecular biological manipulations were performed using standard techniques, as described in Ref. 26.

Glycerol Transport Assays—For glycerol efflux measurements, the cells were cultured in YNB supplemented with 2% glucose to mid log phase (typically $A_{600\ nm}$ = 0.4–0.5). To achieve maximal internal glycerol accumulation, the cells expressing *FPS1* were then incubated for 2–3 h in YNB supplemented with 2% glucose and 5% NaCl, whereas cells expressing *glpF* were incubated for 5–6 h in the NaCl-containing medium. The cells were harvested and suspended in YNB supplemented with 2% glucose at t = 0. The samples (5 ml) were harvested at t = 0, 1, 2, 3, 5, and 10 min, and glycerol efflux was measured as a function of time as described previously (8). Glycerol concentrations were determined enzymatically using a commercially available kit (Roche Molecular Biochemicals).

To determine glycerol influx, the cells were cultured in YNB supplemented with 2% glucose to log phase (typically $A_{600\ nm}$ = 0.7–0.8). The cells were harvested by centrifugation, washed, and suspended in ice-cold MES buffer (10 mM MES, pH 6.0) to a density of 60 mg/ml. Glycerol influx was then measured as described previously (7, 8) by withdrawing 50-μl aliquots and collecting cells by filtration. In each case, the dry weight was determined by harvesting cells on filters, which were then dried at 80 °C to constant weight.

All transport experiments were performed a minimum of three times, and the data were expressed as the mean values at each time point ± S.E. A standard two-tailed unpaired t test was used to test for significant differences between the means, as necessary. In general, transport data were not related to expression levels to give specific activities because the standard error associated with membrane protein expression levels was much higher than that of the transport assays themselves. Hence it was felt that such adjustment is misleading, as has previously been reported in studies where levels in isolated membranes do not reflect those in whole cells (27).

Membrane Preparation and Immunoblots—The cells were cultured in YNB supplemented with 2% glucose to late log phase (typically $A_{600\ nm}$ = 0.8), and both the total membrane and plasma membrane fractions were isolated and visualized as described previously (8).

Molecular Modeling—Models of the A70S mutation in GlpF were generated by extraction of the Cα atom coordinates of *E. coli* GlpF from the Brookhaven Protein Data Bank file, 1FX8, using Molscript commands in RASMOL version 2.7.2 (28). The mutant model was subsequently constructed using the MaxSprout algorithm (29), following substitution of Ala for Ser in the Cα coordinates file. The coordinates for Ser^{70} were then returned to the original file, substituting the Ala^{70} coordinates, resulting in a file that was identical to the original GlpF Brookhaven Protein Data Bank file, except for the additional oxygen atom of the serine residue. Hydrogen bonding was predicted using Swiss-PDB Viewer (30). The amino acid sequences for yeast Fps1p and *E. coli* GlpF were aligned using CLUSTALW (31). Models of the Fps1p pore were generated by extraction of the Cα atom coordinates of the GlpF structure, replacement with corresponding amino acid residues of the aligned Fps1p sequence, and reconstruction of the pore using the MaxSprout algorithm. The regions of changed secondary structure were corroborated by analysis of the Fps1p sequence using the α-helix indices of Chou and Fasman (32) and Deleage and Roux (32, 33) and by analysis of the modeled structure using TMAlpha (34).

RESULTS

Changing NPS and/or NLA to NPA in Fps1p Does Not Affect Glycerol Transport—Fps1p differs from the vast majority of its family members in that it contains NPS and NLA, respectively, in loops B and E (Fig. 1), rather than the signature sequences of the family: two NPA motifs. We began our analysis by restoring these amino acid triplets both singly and doubly to NPA. The mutant genes were expressed from a multi-copy plasmid under the control of the *FPS1* promoter in a yeast strain lacking *FPS1*. The localization of the resultant mutant proteins was examined by cell fractionation and immunoblot. Fig. 2*A* indicates that wild type Fps1p and the three mutants were equally localized to the plasma membrane. Glycerol efflux was assayed by measuring the export of intracellularly produced glycerol, whereas influx was measured following the exposure of cells to radiolabeled glycerol. We observed no statistically significant reduction in glycerol efflux compared with the wild type (Fig. 2*B*) for any of our mutant channels. This was consistent with the growth phenotypes shown in Fig. 2*C*. In these tests, yeast cells with a channel that can export glycerol survive a hypo-osmotic shock, whereas a smaller fraction of yeast cells survive this treatment and also resume growth more slowly in the absence of a functional channel (8). Hence we observed that cells with the mutant channels Fps1p S354A, Fps1p L481P, and Fps1p S354A L481P survived indistinguishably from cells with a wild type channel. Table II shows that the initial glycerol uptake rates for the mutant channels were also not significantly different from the wild type, with rates in the range of 85–116% of the mean wild type value. This confirmed that changing NPS and/or NLA to NPA in Fps1p does not substantially affect its glycerol transport properties. In addition, we note that cells with mutant channels did not show any growth defect in high osmolarity medium such as 1 M sorbitol (Fig. 2*C*) or high salt (not shown), which would otherwise indicate changes in channel regulation.

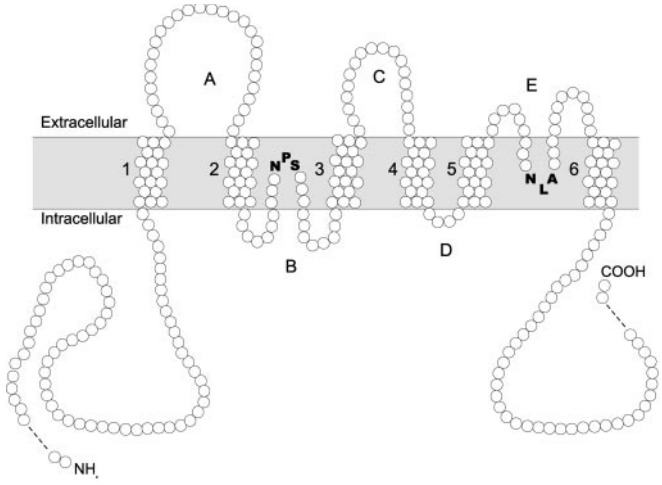

FIG. 1. **Schematic diagram of Fps1p.** Fps1p differs from more typical members of the MIP family, such as GlpF, in a number of ways. For example the signature NPA motifs of the family are replaced by NPS and NLA in Fps1p, as indicated. The *numbers* indicate the six transmembrane domains. The *letters A–E* denote the loops of Fps1p, of which B and E are involved in the formation of the glycerol channel by dipping into the membrane to form an hourglass. The *dashed lines* within the amino- and carboxyl-terminal extensions indicate that they are much longer than shown (256 and 143 amino acids, respectively). The membrane core comprises 270 amino acids.

Changing NPA to NPS and/or NLA in GlpF Affects Glycerol Transport—It was clear from the experiments described above that in our assays neither NPS nor NLA is specifically required for apparently normal glycerol transport by Fps1p. To begin to understand this observation, we examined the functional consequences of converting the NPA to NPS and/or NLA in GlpF, which is a more typical member of the MIP family in terms of sequence. We have shown previously that GlpF, which is the closest bacterial homolog of Fps1p, can be functionally expressed in *S. cerevisiae*. Although cells expressing the unregulatable GlpF channel initially lose glycerol and are slightly osmosensitive (8), we observed that after prolonged incubation GlpF-expressing transformants did accumulate glycerol in hyperosmotic medium (7). This allowed the GlpF constructs to be tested in exactly the same way as the Fps1p mutants described above.

We therefore constructed NPA to NPS in loop B (A70S), as well as NPA to NLA in loop E (P204L) and the double NPS/NLA mutant (A70S P204L). These mutants were analyzed by cell fractionation and immunoblot for localization (Fig. 3*A*) and in both our efflux (Fig. 3*B*) and influx (Table II) assays. In

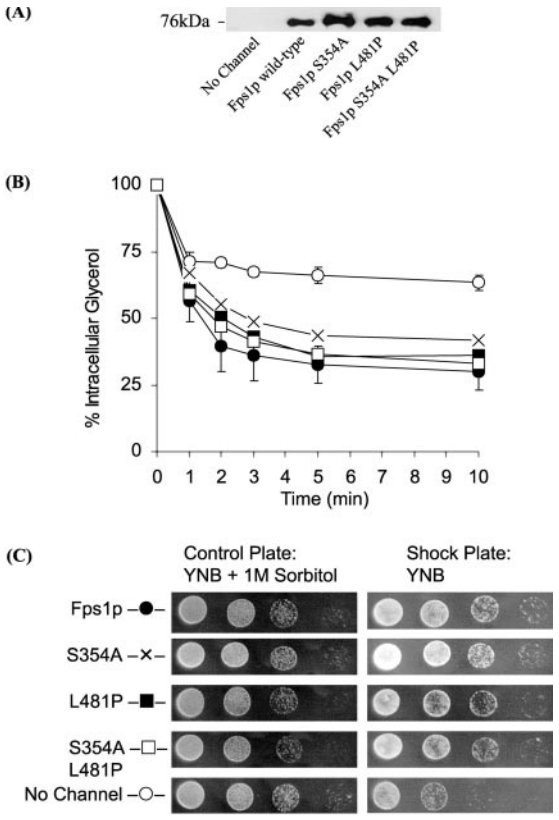

FIG. 2. **Functional analysis of point mutants of Fps1p.** *A*, Western blots of plasma membrane extracts. Representative blots are shown. *B*, glycerol transport measurements on whole yeast cells were performed in triplicate for efflux to determine the transport characteristics of cells with either Fps1p (●), no glycerol channel (○), Fps1p S354A (×), Fps1p L481P (■), or Fps1p S354A L481P (□). The mean values are presented ± S.E. (n = 3). *C*, growth characteristics following hypo-osmotic shock are consistent with the efflux properties of the mutant proteins. The cells were spotted onto plates in a 10-fold serial dilution series such that they experienced either no shock (*left panel*) or a hypo-osmotic shock (*right panel*).

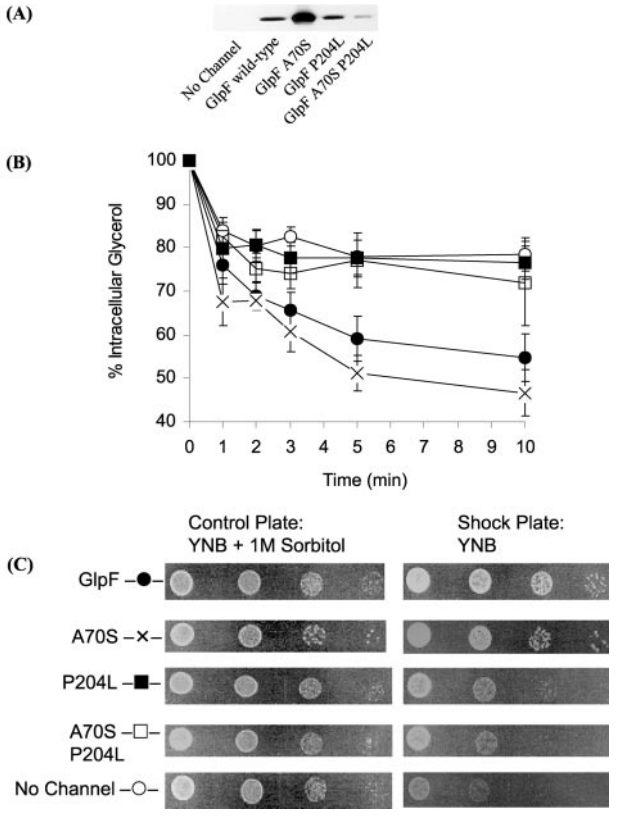

FIG. 3. **Functional analysis of point mutants of GlpF.** *A*, Western blots of plasma membrane extracts. Representative blots are shown. *B*, glycerol transport measurements on whole yeast cells were performed in triplicate for efflux to determine the transport characteristics of cells with either GlpF (●), no glycerol channel (○), GlpF A70S (×),GlpF P204L (■), or GlpF A70S P204L (□). The mean values are presented ± S.E. (n = 3). *C*, growth characteristics following hypo-osmotic shock are consistent with the efflux properties of the mutant proteins. The cells were spotted onto plates in a 10-fold serial dilution series such that they experienced either no shock (*left panel*) or a hypo-osmotic shock (*right panel*).

TABLE II
Initial glycerol uptake rates

Values were obtained from triplicate determinations as described under "Experimental Procedures." The rates are expressed as the means ± S.E. (n = 3).

Protein	Initial uptake rate
	nmol/mg/min
No channel	1.03 ± 0.08
Fps1p	4.20 ± 0.19
Fps1p S354A	3.85 ± 0.18
Fps1p L481P	3.55 ± 0.40
Fps1p S354A L481P	4.87 ± 0.45
GlpF	2.88 ± 0.35
GlpF A70S	2.16 ± 0.23
GlpF P204L	1.16 ± 0.19
GlpF A70S P204L	1.10 ± 0.08
GlpF loop B swap	1.54 ± 0.28
GlpF loop E swap	1.16 ± 0.31
GlpF loops B and E swap	1.15 ± 0.07

contrast to the Fps1p series, we observed that mutations in GlpF affected protein localization differently in each case. GlpF A70S was expressed on average at higher levels than wild type, GlpF P204L was expressed at wild type levels, and the double mutant, GlpF A70S P204L, was poorly expressed (Fig. 3*A*). With respect to our transport assays (Fig. 3*B* and Table II), GlpF A70S showed substantial activity, having 75% of the mean uptake rate of wild type GlpF and approximately wild type export activity. Given the apparent higher expression level, this may indicate a reduced specific transport activity per channel. However, transport proficiency of this mutant was supported by growth phenotypes; cells with the mutant channel A70S and the wild type channel survived a hypo-osmotic shock, indicating that only these channels were functional (Fig. 3*C*). For GlpF P204L, this nonconservative mutation in loop E apparently resulted in a properly localized but essentially nonfunctional protein. Similarly, the double mutant was also nonfunctional, although at least some protein appeared to be localized to the plasma membrane. From these observations we concluded that the pores of Fps1p and GlpF were not structurally identical; although Fps1p containing two NPA motifs appeared to have wild type properties in our assays (Fig. 2), the reverse was not true for GlpF, because only NPS in loop B could be tolerated in the GlpF pore (Fig. 3).

Loops B and E of Fps1p Do Not Form a Functional Channel in GlpF—The apparent inability of GlpF to tolerate NLA in loop E indicated that there might be sequences in the B and E loops of Fps1p that are required if the interaction of these NPS- and NLA-containing loops are to form a fully functional channel in GlpF. We therefore precisely aligned the sequences of Fps1p and GlpF using the internet resources, Prosis, TopPred2, TMPred, PhD, and DAS, together with structural information for GlpF (18), and transferred the predicted loops B and E from Fps1p to GlpF both singly and doubly, to make GlpF even more Fps1p-like. None of these mutants conferred any

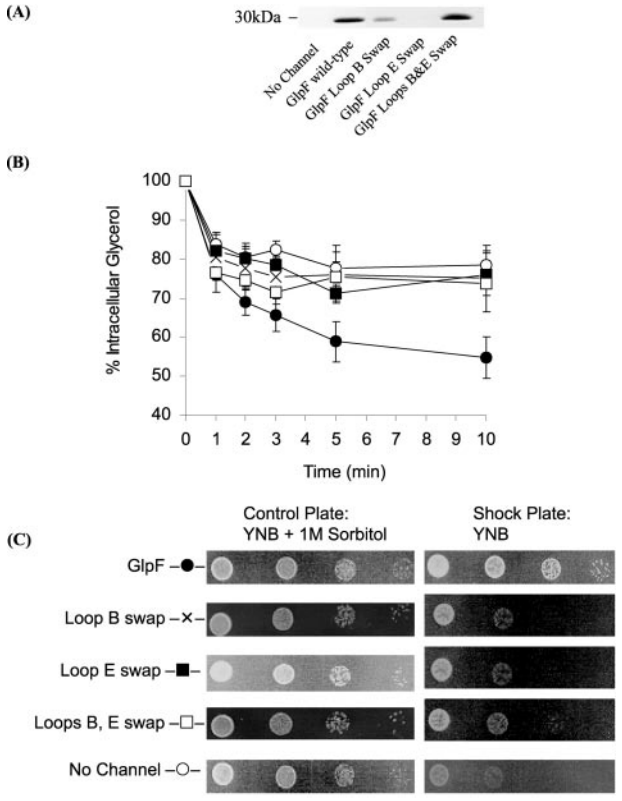

FIG. 4. **Functional analysis of loop swap mutants of GlpF.** *A*, Western blots of plasma membrane extracts. Representative blots are shown. *B*, glycerol transport measurements on whole yeast cells were performed in triplicate for efflux to determine the transport characteristics of cells with either GlpF (●), no channel (○), GlpF in which loop B had been exchanged for that of Fps1p (×), GlpF in which loop E had been exchanged for that of Fps1p (■), or GlpF in which both loops B and loop E had been exchanged for those of Fps1p (□). The mean values are presented ± S.E. (n = 3). *C*, growth characteristics following hypo-osmotic shock are consistent with the efflux properties of the mutant proteins. The cells were spotted onto plates in a 10-fold serial dilution series such that they experienced either no shock (*left panel*) or a hypo-osmotic shock (*right panel*).

glycerol transport activity (Fig. 4 and Table II). For the E-loop swap, in particular, this is probably because it was not properly expressed or localized to the plasma membrane. The double loop swap was expressed to wild type levels but was nonfunctional, indicating that GlpF could not tolerate the channel-forming loops of Fps1p. Again, growth tests confirmed the biochemical analyses of the channels; only cells with the wild type channel survived a hypo-osmotic shock, indicating that only this channel confers glycerol export (Fig. 4*C*). These observations indicate that in addition to loops B and E, other sequences, probably within the transmembrane domains, contribute to functional differences between Fps1p and GlpF.

DISCUSSION

Our mutational studies and analyses in whole yeast cells have shown that Fps1p can tolerate conventional MIP channel NPA motifs. Changing NPS in loop B and NLA in loop E either singly or doubly into NPA either did not affect, or only marginally affected, localization and function of the mutant protein. We noted that although the single Fps1p mutants had somewhat reduced activities compared with wild type, the double mutant was wild type-like (Table II). In contrast, making the reverse mutations in the prototypic MIP glycerol facilitator, GlpF, had pronounced effects. Although NPS in loop B affected but did not abolish function, the presence of NLA in loop E or the swapping of loops B and/or E of Fps1p to GlpF abolished function and also affected localization to the plasma membrane. These observations indicated that the pores of the two glycerol facilitators, Fps1p and GlpF, are different.

To rationalize our experimental observations, we generated a model of the transmembrane core of Fps1p based on the aligned regions of the GlpF structure reported by Fu and colleagues (18). Fig. 5 indicates marked differences between the pore regions of GlpF and Fps1p. In particular, Fps1p contains significantly less α-chain around the inner part of the pore. Consequently, our observations can be rationalized in terms of the comparatively greater flexibility of the Fps1p pore with respect to GlpF. By comparing the sequences flanking the NPA of loop E of GlpF with the corresponding NLA in Fps1p, it is clear that the latter also contribute to this flexibility. Specifically, it appears that the GlpF sequence PLTGFAMNPARD provides for a strong α-helix between the prolines, whereas the equivalent Fps1p sequence QTGTAAMNLARD has no such provision. Another consequence of the lower α-helical content is that the region where loops B and E approach each other in Fps1p, Ser^{354}/Asn^{480}, is more exposed than the equivalent Ala^{70}/Asn^{203} in GlpF.

It is possible that the minor reduction in initial glycerol uptake rate for Fps1p S354A is due to disruption of the polar environment of the pore, because alanine is both bulkier and less polar than serine. In particular potential hydrogen bonding between Ser^{354} and Glu^{377} of transmembrane domain 3 would be abolished. For Fps1p L481P, the slight reduction in initial glycerol uptake rate may be due to loop E becoming less flexible in a region crucial for transport activity. In addition, hydrogen bonding may again be affected; the introduction of a proline reduces the potential for hydrogen bonding within the pore, which might be important for maintaining optimal pore architecture and loop/helix proximities. Interestingly, the double mutant Fps1p S354A L481P has a wild type-like initial glycerol uptake rate. In this case the mutant channel contains the MIP family signature NPA/NPA sequence. It appears that in the absence of the Ser^{354}/Glu^{377} interaction, the double mutation causes a realignment of polar groups and hydrogen bonding within the pore. This compensates for the loss of the serine and allows efficient tracking of the substrate through the pore. For instance, it is likely that Asn^{480} on loop E can come closer to Asn^{352} on loop B, allowing the formation of a favorable hydrogen bond. Hence in the case of Fps1p, NPA/NPA functions as well as NPS/NLA, suggesting that overall, the ability of a pore to transport glycerol appears to be a balance between polarity and stabilizing hydrogen bonds within the pore itself.

In GlpF, we observed that modifications restricting the already limited pore flexibility resulted in a significant reduction in transport function. In particular, our model of GlpF A70S (Fig. 6) based on the coordinates of the GlpF structure (18) may be used to rationalize the apparently somewhat reduced transport rates incurred by the mutation (taking into account the apparently increased expression level of this construct). The introduction of a serine residue at position 70 appears to result in slightly reduced flexibility of Asn^{68} because of increased hydrogen bonding between the side chain oxygen atom of Ser^{70} and the side chain nitrogen of Asn^{68} (4.16 Å apart). However, these effects are likely to be offset by an increased polar environment within the pore, resulting in only small effects on transport. In contrast, transport function in GlpF is significantly compromised by other substitutions, such as the loop E P204L substitution. This is likely to involve the role of proline as a "helix breaking" residue, its loss in the mutant leading to a lengthened helical section in loop E, incorporating the mutant NLA motif. This alteration most probably significantly

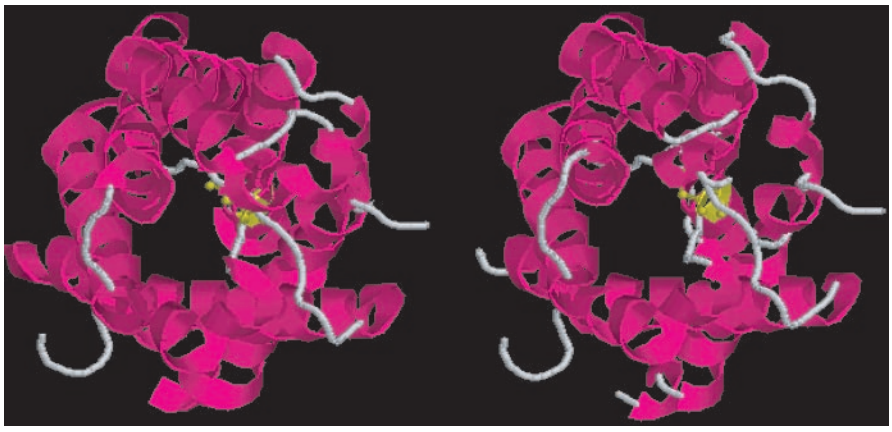

FIG. 5. **Homology model of the Fps1p pore region (*right*) based on the structure of GlpF (*left*) displayed in RASMOL.** The Fps1p pore displays markedly less α conformation (shown in *pink*), resulting in a more flexible structure. The higher degree of random conformation (shown in *white*) is most evident around the inner pore, particularly in the region of the Ser^{354}/Asn^{480} loop B/loop E approach (shown in *yellow*), which is subsequently more exposed than the equivalent Ala^{70}/Asn^{203} in GlpF.

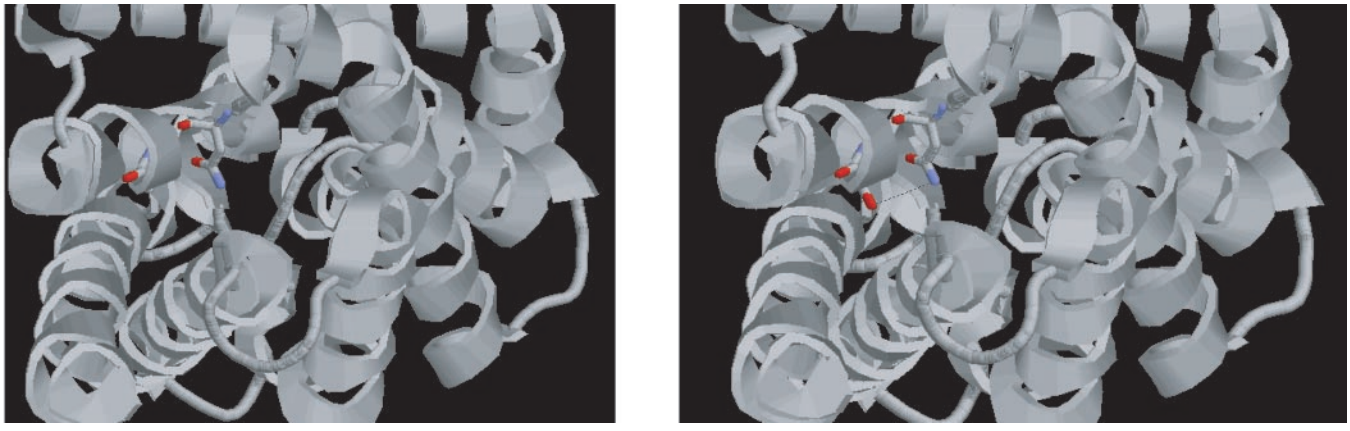

FIG. 6. **Modeling of the A70S mutation in GlpF, displayed in RASMOL.** The wild type is shown in the *left panel*, with Asn^{68} (*center*) and Ala 70 (*left*) rendered. The A70S form is shown in the *right panel* and displays the probable hydrogen bond formation (*black line*) between Asn^{68} and Ser^{70} because of the additional side chain oxygen of Ser^{70}, limiting the flexibility of Asn^{68}.

reduces the flexibility of the surrounding amino acids, compared with the situation when an NPA motif is present.

In summary, it is clear that the pores of GlpF and Fps1p are different, even though both proteins are members of the "glycerol facilitator" subfamily of the MIP superfamily. The rigid pore of GlpF is sensitive to changes in its signature NPA motifs and cannot accommodate the B and E loops of Fps1p, whereas the pore of Fps1p is more permissive to change. Hence, it is probable that the presence of NPS and NLA, rather than the more typical NPA and NPA, in the pore of Fps1p are tolerated by the more flexible structure.

Why have these two glycerol facilitators evolved different pore designs? A possible explanation may be the fact that Fps1p and GlpF have different physiological roles. Although Fps1p appears to be implicated in the export of glycerol during osmoadaptation (7, 9), GlpF functions in the uptake of glycerol from the growth medium as a first step to catabolize it as a source of carbon and energy (14, 35). However, in addition to their common glycerol transport functions, Fps1p and GlpF each have other unique roles. Fps1p is gated rapidly by changes in medium osmolarity (8) to prevent glycerol leakage and to ensure appropriate intracellular glycerol accumulation. GlpF, on the other hand, interacts with glycerol kinase to ensure rapid glycerol phosphorylation, thereby preventing any glycerol taken up being lost again by diffusion out of the cell (15). We do not yet understand the mechanism that mediates gating in Fps1p, although we have shown previously that certain parts of the amino-terminal extension are needed for channel closing (8). We have also observed that addition of these sequences to GlpF, which is unregulated, is not sufficient for its gating, resulting in a protein with properties that are indistinguishable from wild type GlpF.[2] What is clear, however, is that Fps1p responds within seconds to osmotic stress (8), suggesting a conformational change is involved in gating. The flexible pore of Fps1p could be permissive to such a conformational change leading to closure of the pore by a mechanism that remains to be identified. Structural modeling, as employed in this study, may aid us in achieving a better understanding of this mechanism.

A more flexible pore may also have consequences for transport specificity. Although both proteins appear to transport a similar spectrum of smaller polyols (18),[3] different transport capacities of Fps1p and GlpF for the polyol-like oxoanions of As(III) and Sb(III) have been reported. Fps1p has been shown to mediate the uptake of As(III) and Sb(III) into *S. cerevisiae*. Through the regulation of this uptake, the channel has been suggested to have a role in toxic metalloid resistance in yeast (36). In the same study, no equivalent uptake could be demonstrated for GlpF, although GlpF has already been suggested to transport Sb(III), but not As (III), in *E. coli* (16), thus indicating a specificity difference between these close homologs. This hypothesis awaits a more thorough functional analysis of the transport specificity of Fps1p, which is currently in progress. Comparison of these data with data emerging on the recently identified, but as yet uncharacterized, homologs of Fps1p from different yeast species (natchaug.labri.u-bordeaux.fr/Genolevures/Genolevures.php3) should shed light on the intriguing presence of atypical signature motifs in these unusual MIP family members.

[2] R. M. Bill and S. Hohmann, unpublished observations.
[3] S. Karlgren, R. M. Bill, and S. Hohmann, unpublished observations.

Acknowledgments—We thank Dr. Cândida Lucas (Universidade do Minho, Braga, Portugal) and Dr. Markus Tamás (Göteborg University) for helpful discussions and Aleksandras Gutmanas (Göteborg University) for assistance with Figs. 5 and 6.

REFERENCES

1. Borgnia, M., Nielsen, S., Engel, A., and Agre, P. (1999) *Annu. Rev. Biochem.* **68,** 425–458
2. Johansson, I., Karlsson, M., Johanson, U., Larsson, C., and Kjellbom, P. (2000) *Biochim. Biophys. Acta* **1465,** 324–342
3. Kuwahara, M., Ishibashi, K., Gu, Y., Terada, Y., Kohara, Y., Marumo, F., and Sasaki, S. (1998) *Am. J. Physiol.* **275,** C1459–C1464
4. Deen, P. M., and Knoers, N. V. (1998) *Curr. Opin. Nephrol. Hypertens.* **7,** 37–42
5. Kaldenhoff, R., Grote, K., Zhu, J. J., and Zimmermann, U. (1998) *Plant J.* **14,** 121–128
6. Kjellbom, P., Larsson, C., Johansson, I., Karlsson, M., and Johanson, U. (1999) *Trends Plant Sci.* **4,** 308–314
7. Luyten, K., Albertyn, J., Skibbe, W. F., Prior, B. A., Ramos, J., Thevelein, J., and Hohmann, S. (1995) *EMBO J.* **14,** 1360–1371
8. Tamás, M. J., Luyten, K., Sutherland, F. C. W., Hernandez, A., Albertyn, J., Valadi, H., Li, H., Prior, B. A., Kilian, S. G., Ramos, J., Gustafsson, L., Thevelein, J. M., and Hohmann, S. (1999) *Mol. Microbiol.* **31,** 1087–1104
9. Tamás, M. J., Rep, M., Thevelein, J. M., and Hohmann, S. (2000) *FEBS Lett.* **472,** 159–165
10. Tao, W., Deschenes, R. J., and Fassler, J. S. (1999) *J. Biol. Chem.* **274,** 360–367
11. Hohmann, S., Bill, R. M., Kayingo, G., and Prior, B. A. (2000) *Trends Microbiol* **8,** 32–36
12. Sutherland, F. C., Lages, F., Lucas, C., Luyten, K., Albertyn, J., Hohmann, S., Prior, B. A., and Kilian, S. G. (1997) *J. Bacteriol.* **179,** 7790–7795
13. Holst, B., Lunde, C., Lages, F., Oliveira, R., Lucas, C., and Kielland-Brandt, M. C. (2000) *Mol. Microbiol.* **37,** 108–124
14. Sweet, G., Gandor, C., Voegle, R., Wittekindt, N., Beuerle, J., Truniger, V., Lin, E. C. C., and Boos, W. (1990) *J. Bacteriol.* **172,** 424–430
15. Voegele, R. T., Sweet, G. D., and Boos, W. (1993) *J. Bacteriol.* **175,** 1087–1094
16. Sanders, O. I., Rensing, C., Kuroda, M., Mitra, B., and Rosen, B. P. (1997) *J. Bacteriol.* **179,** 3365–3367
17. Jung, J. S., Preston, G. M., Smith, B. L., Guggino, W. B., and Agre, P. (1994) *J. Biol. Chem.* **269,** 14648–14654
18. Fu, D., Libson, A., Miercke, L. J., Weitzman, C., Nollert, P., Krucinski, J., and Stroud, R. M. (2000) *Science* **290,** 481–486
19. Murata, K., Mitsuoka, K., Hirai, T., Walz, T., Agre, P., Heymann, J. B., Engel, A., and Fujiyoshi, Y. (2000) *Nature* **407,** 599–605
20. Thomas, B. J., and Rothstein, R. (1989) *Cell* **56,** 619–630
21. Berben, G., Dumont, J., Gilliquet, V., Bolle, P. A., and Hilger, F. (1991) *Yeast* **7,** 475–477
22. Sherman, F., Fink, G. R., and Hicks, J. B. (1983) *Methods in Yeast Genetics*, Cold Spring Harbor Laboratory, Cold Spring Harbor, NY
23. Sarkar, G., and Sommer, S. *S. (1990) BioTechniques* **8,** 404–407
24. Ito, H., Funkuda, Y., Murata, K., and Kimura, A. (1983) *J. Bacteriol.* **153,** 163–168
25. Muhlrad, D., Hunter, R., and Parker, R. (1992) *Yeast* **8,** 79–82
26. Sambrook, J., Fritsch, E. F., and Maniatis, T. (1989) *Molecular Cloning: A Laboratory Manual*, Cold Spring Harbor Laboratory Press, Cold Spring Harbor, NY
27. Cain, S. M., Matzke, E. A., and Brooker, R. J. (2000) *J. Membr. Biol.* **176,** 159–168
28. Sayle, R. A., and Milner-White, E. J. (1995) *Trends Biochem. Sci.* **20,** 374
29. Holm, L., and Sander, C. (1991) *J. Mol. Biol.* **218,** 183–194
30. Guex, N., and Peitsch, M. C. (1997) *Electrophoresis* **18,** 2714–2723
31. Thompson, J. D., Higgins, D. G., and Gibson, T. J. (1994) *Nucleic Acids Res.* **22,** 4673–4680
32. Chou, P. Y., and Fasman, G. D. (1978) *Adv. Enzymol. Relat. Areas Mol. Biol.* **47,** 45–148
33. Deleage, G., and Roux, B. (1987) *Protein Eng.* **1,** 289–294
34. Sarakinou, K. S., Antoniw, J. F., Togawa, R. C., and Mullins, J. G. L. (2001) *Biochem. Soc. Trans.* **29,** 36
35. Heller, K. B., Lin, E. C., and Wilson, T. H. (1980) *J. Bacteriol.* **144,** 274–278
36. Wysocki, R., Chery, C. C., Wawrzycka, D., Van Hulle, M., Cornelis, R., Thevelein, J. M., and Tamás, M. J. (2001) *Mol. Microbiol.* **40,** 1391–1401

Analysis of the Pore of the Unusual Major Intrinsic Protein Channel, Yeast Fps1p

Roslyn M. Bill, Kristina Hedfalk, Sara Karlgren, Jonathan G. L. Mullins, Jan Rydström and Stefan Hohmann

J. Biol. Chem. 2001, 276:36543-36549.
doi: 10.1074/jbc.M105045200 originally published online July 9, 2001
